Structural implications for heavy metal-induced reversible assembly and aggregation of a protein: the case of *Pyrococcus horikoshii* CutA[1]

Yoshikazu Tanaka[a], Kouhei Tsumoto[a,*], Takeshi Nakanishi[a], Yoshiaki Yasutake[b], Naoki Sakai[b], Min Yao[b], Isao Tanaka[b], Izumi Kumagai[a,**]

[a] *Department of Biomolecular Engineering, Graduate School of Engineering, Tohoku University, Aoba-yama 07, Aoba-ku, Sendai 980-8579, Japan*
[b] *Division of Biological Sciences, Graduate School of Science, Hokkaido University, Sapporo 060-0810, Japan*

Received 8 October 2003; revised 17 November 2003; accepted 18 November 2003

First published online 8 December 2003

Edited by Hans Eklund

Abstract **CutA is a small protein that appears to be involved in the mechanism of divalent metal cation tolerance in microorganisms. Here we report the crystal structure of *Pyrococcus horikoshii* CutA (*Pho*CutA), with and without Cu^{2+}, and its metal-binding properties. Crystallographic analyses revealed that *Pho*CutA forms a stable trimeric structure with intertwined antiparallel β-strands. The crystal structure of the Cu^{2+}–*Pho*CutA complex shows that the Cu^{2+} is located at a trimer–trimer interface and is recognized by the side chains of one Asp^{48} from each trimer. In an in vitro experiment, *Pho*CutA bound to several heavy metals, most of which led to reversible aggregation of the protein; i.e. the aggregates could be completely solubilized by addition of ethylenediamine tetraacetic acid (EDTA) or dialysis against metal free buffer. Substitution of Asp^{48} with Ala led to a decrease in the amount of aggregates, suggesting the significant contribution of Asp^{48} to the reversible aggregation. To the best of our knowledge, this is the first report which provides the structural evidence for heavy metal-induced multimerization of a protein.**

Key words: CutA; *Pyrococcus horikoshii*; Crystal structure; Heavy metals; Multimerization; Reversible aggregation

1. Introduction

Heavy metals play numerous critical roles in various biological processes, e.g. as cofactors of enzymes, as stabilizers of protein structures, and in maintenance of osmotic balance [1–3]. Excess heavy metals, however, are harmful to cells, resulting in cell death through their binding to essential cellular components [4]. Therefore, the intracellular concentrations of heavy metals have to be controlled tightly.

In microorganisms, resistance to heavy metals is mediated by a series of systems encoded by chromosomal and plasmid DNAs, and six resistance mechanisms have been reported, i.e. exclusion of metals by a permeability barrier, intra- and extracellular sequestration of metals, active transport efflux pumps, enzymatic detoxification, and reduction in the sensitivity of cellular targets to metal ions [5]. Among these mechanisms, active transport efflux pumps constitute the largest category.

The *cop* genes and *cut* genes appear to be associated with the system that regulates copper levels. Four genes, *copA*, *copB*, *copY*, and *copZ*, occur in the *cop* operon [6]; their products and functions are CopA: uptake adenosine triphosphatase (ATPase); CopB: efflux ATPase [7]; CopY and CopZ: regulators of the *cop* operon [8]. This is a well-understood system of active transport efflux pumps. There are six *cut* genes, *cutA*, *cutB*, *cutC*, *cutD*, *cutE*, and *cutF* [9], but the functions of only CutC, CutE, and CutF have been examined or presumed. CutE has been identified as an intracellular copper-binding protein [10], and it seems to function as an apolipoprotein *N*-acyltransferase [11]. CutF is an outer membrane lipoprotein, and apo-CutF is attached to fatty acids by CutE [12,13]. CutE may therefore have an effect on the copper permeability of bacterial cells. Sequence analysis revealed that CutC contains a MPRMEDIM sequence, which is similar to the copper-binding motif MXXXXMXXM [12], and thus CutC may be a cytoplasmic copper-binding protein. In contrast to CutC, CutE, and CutF, the functions of CutA, CutB, and CutD are still not clear; so the details of the Cut system have not yet been clarified.

The *cutA* gene is universally distributed in a wide variety of bacteria, and its product CutA is a relatively small protein of molecular mass about 12 kDa. Based on genetic analyses of *Escherichia coli*, CutA has been proposed to be related to the copper tolerance mechanism [14]. As mentioned above, however, the function of this protein has not yet been clarified.

Here we report the crystal structure of CutA from the hyperthermophilic archaeon *Pyrococcus horikoshii* (*Pho*CutA), with and without bound Cu^{2+}. Metal-mediated interactions between *Pho*CutA trimers suggested that the protein may associate into multimers in the presence of metal ions, and additional experiments revealed that some metal ions lead to multimerization and precipitation of *Pho*CutA and that these phenomena are reversible. On the basis of these observations,

*Corresponding author. Fax: (81)-22-217-7276.
**Corresponding author. Fax: (81)-22-217-6164.
E-mail addresses: tsumoto@mail.cc.tohoku.ac.jp (K. Tsumoto), kmiz@mail.cc.tohoku.ac.jp (I. Kumagai).

[1] The atomic coordinates of *Pyrococcus horikoshii* (*Pho*)CutA and the Cu^{2+}–*Pho*CutA complex have been deposited in the Protein Data Bank under the accession numbers 1J2V and 1UKU for *Pho*CutA and Cu^{2+}–*Pho*CutA, respectively.

Abbreviations: SDS, sodium dodecyl sulfate; PAGE, polyacrylamide gel electrophoresis; *Pho*CutA, *Pyrococcus horikoshii* CutA; Se-Met, selenomethionine

0014-5793/03/$30.00
doi:10.1016/S0014-5793(03)01402-9

we discuss the biological and chemical implications of metal-binding properties of *Pho*CutA.

2. Materials and methods

2.1. Construction of Pho*CutA, L26M mutant, and D48A mutant expression vectors*

The gene encoding *Pho*CutA was amplified by KOD-Plus DNA polymerase (Toyobo), using *P. horikoshii* genomic DNA as a template and the following designed primers. *Nde*I and *Bam*HI sites were incorporated into PH0992back (5′-GGAATTCCATATGATAAT-AGTTTACACGACTTTTCCGGAC-3′) and PH0992forward (5′-C-GCGGATCCTCATTTTTTCGTCTCTTCAATTAACCATTTG-3′), respectively (restriction enzyme sites are underlined). The polymerase chain reaction (PCR) products were inserted into the pET20b vector (Novagen). Substitution of Leu^{27} with Met was performed by PCR using the PH0992back, PH0992forward, and synthesized primers (5′-TTAAAAGAGAGGATGATTGCATGCGC-3′ and 5′-GCGCAT-GCAATCATCCTCTCTTTTAA-3′, mutated sites are underlined). Substitution of Asp^{48} with Ala was performed by PCR using the PH0992back, PH0992forward, and synthesized primers (5′-ATC-GAGGAAGCTAAAGAAGTT-3′ and 5′-AACTTCTTTAGCTTC-CTCGAT-3′, mutated sites are underlined).

2.2. Expression, purification, and crystallization

A transformed *E. coli* strain, BL21(DE3), harboring an expression vector was grown at 37°C in Luria–Bertani (LB) medium supplemented with 100 μg ml^{-1} ampicillin until the early stationary phase. To induce expression of *Pho*CutA, isopropyl β-D-thiogalactopyranoside (IPTG) was added to a final concentration of 1 mM, and the culture was grown for 3 h at 37°C. The selenomethionine (Se-Met) derivative of *Pho*CutA was expressed in a methionine auxotroph *E. coli* strain, B834(DE3) transformed with pET20b/PH0992L26M, grown in M9 medium supplied with Se-Met. Cells were harvested by centrifugation at 5000×*g* for 10 min at 4°C, washed with 50 mM Tris–HCl (pH 8.0), 50 mM NaCl, and then resuspended in the same buffer. The suspension was sonicated, and then centrifuged at 8000×*g* for 30 min at 4°C. The soluble fraction was incubated at 70°C for 30 min, and then centrifuged at 8000×*g* for 30 min at 20°C. The resulting supernatant was loaded onto a HiTrap QXL column (Amersham Bioscience), previously equilibrated with 50 mM Tris–HCl (pH 8.0). The column was washed with 50 mM Tris–HCl (pH 8.0); then the adsorbed protein was eluted with 75 ml of a 0–0.8 M gradient of NaCl in 50 mM Tris–HCl. Fractions eluting at 45–55 ml were further purified on a HiLoad 26/60 Superdex 75 pg column (Amersham Bioscience), equilibrated with 50 mM Tris–HCl (pH 8.0) containing 200 mM NaCl. Fractions eluting at 165–175 ml were loaded onto a ResourceQ column (Amersham Bioscience), previously equilibrated with 50 mM Tris–HCl (pH 8.0), and adsorbed protein was eluted with 40 ml of a 0.3–0.8 M gradient of NaCl in 50 mM Tris–HCl (pH 8.0).

The initial crystallization conditions were screened by the sparse matrix method at 20°C, using a Crystal Screen kit (Hampton Research). Crystals of *Pho*CutA most suitable for further analyses could be grown from 100 mM acetate buffer (pH 4.6) containing 1.6 M ammonium sulfate by the hanging-drop vapor-diffusion method. Crystals of the *Pho*CutA–Cu^{2+} complex were grown from 100 mM acetate buffer (pH 4.4), 1.5 M ammonium sulfate, 2 mM $CuSO_4$ by the hanging-drop vapor-diffusion method.

2.3. Diffraction data collection and processing

All X-ray diffraction data sets for *Pho*CutA were collected at the third-generation synchrotron radiation facility, SPring-8 (Harima, Japan), under cryogenic conditions. The diffraction experiment for the Se-Met-substituted crystal of *Pho*CutA was performed on the beamline BL41XU. Three wavelengths were chosen on the basis of the fluorescence spectrum of the Se K absorption edge, corresponding to the maximum f'' (peak, 0.9792 Å), minimum f' (edge, 0.9794 Å), and the reference point (remote, 0.9000 Å). The three-wavelength MAD data set was collected up to a resolution of 2.0 Å. The data were indexed and integrated with the program MOSFLM [15] and were scaled and merged with the program SCALA within the CCP4 suite [16]. The Se-Met-substituted crystal of *Pho*CutA belongs to space group $P6_3$ with unit cell dimensions $a = b = 52.6$ Å and $c = 58.1$ Å. At this step, the cumulative intensity statistics clearly indicated that the MAD data were obtained from a twinned crystal [17]. The twinning operator was determined, and the twinning fraction was estimated with the program CNS [18]. For the *Pho*CutA–copper complex, the diffraction data up to a resolution of 1.45 Å were collected on the beamline BL38B1 with the 0.9000 Å radiation. The diffraction data were indexed, integrated, scaled, and merged using the HKL2000 program package [20]. The crystal of the copper complex belongs to space group $P321$ with unit cell parameters $a = b = 52.4$ Å and $c = 54.1$ Å.

2.4. Structure solution and refinement

The structure of Se-Met-substituted *Pho*CutA was solved by the MAD method. For the MAD phasing, we used diffraction data that were not detwinned. The program SOLVE/RESOLVE [21–23] was used to calculate the initial phases, to improve the phases by the solvent flattening and maximum likelihood density modification, and to perform automatic model building. The program RESOLVE successfully placed 80 out of 102 residues, which were partly built as polyalanine fragments. The complete atomic model with the total 102 residues, including side chains, was rebuilt manually with the graphic program O [24]. The structure of the *Pho*CutA–copper complex was determined by the molecular replacement (MR) method using the program AMoRe [25], using the structure of Se-Met-substituted *Pho*CutA as a search probe.

The positional and individual *B* factor refinement for two structures was carried out with the program CNS [18] and REFMAC5 [19]. To monitor the refinement, a random 10% subset from all reflections was set aside for calculation of the free *R* factor (R_{free}). For the Se-Met-substituted structure, the twinning operator (h $-h$ $-k$ $-l$) with a fraction of 0.16 was introduced into all stages of model refinement. After iterative cycles of refinement and manual model fitting, the water molecules were automatically located by peak searching on the SigmaA-weighted mF_o–DF_c map, and some water molecules, which occupied irrelevant positions, were deleted on the basis of their real-space correlation coefficient and/or maximum density level using the procedure in the program CNS [18]. Finally, the crystallographic *R* values (R_{free} values) of the Se-Met structure and the copper complex converged to 23.7% (28.9%) and 16.2% (19.4%), respectively. The stereochemical quality of the final refined models was analyzed by the program PROCHECK [26]. The data collection, processing, and refinement statistics are summarized in Table 1. The surface charge of the *Pho*CutA trimer was calculated using the program GRASP [27].

2.5. Analysis of the effects of metal ions

Purified *Pho*CutA was dialyzed against 20 mM Tris–HCl (pH 8.0) containing 2 mM of a metal ion. After 6 h, the protein solutions were centrifuged at 15000×*g* for 30 min. The supernatant and precipitate obtained were added to an equal volume of buffer containing sodium dodecyl sulfate (SDS) (62.5 mM Tris–HCl (pH 6.8), 2.3% (w/v) SDS, 8% (w/v) glycerol, 1.4 M β-mercaptoethanol, 0.1% (w/v) bromophenol blue), followed by incubation at 95°C for 10 min. Each solution was subjected to polyacrylamide gel electrophoresis (PAGE) under reducing conditions and the gel was stained with Coomassie brilliant blue R-250.

3. Results and discussion

3.1. Crystal structure of Pho*CutA*

The structure of *Pho*CutA was solved by the Se-MAD method and was refined to 2.0 Å resolution. The final refined model revealed that *Pho*CutA is a tightly intertwined trimer assembled so as to form a circularly closed β-sheet structure consisting of 15 antiparallel β-strands (five β-strands for each monomer, Fig. 1A and B). Each trimer has three identical intersubunit interfaces, which are predominantly formed by hydrogen bonds among the equivalent β-strands (β2), that is the same strand but on different subunits and between β4 and β5 (Fig. 1A and C). The trimeric structure seems to be additionally stabilized by a hydrophobic core that is constructed from residues Ile^3, Ile^{54}, Ile^{83}, and Val^{85}. This stable trimeric assembly observed in the crystal structure is consistent with

Table 1
Data collection and refinement statistics

	Se-Met-substituted structure (MAD)			Copper complex
	Peak	Edge	Remote	
Data collection				
Space group	$P6_3$			$P321$
Cell dimensions (Å)	$a = b = 52.6$, $c = 58.1$			$a = b = 52.4$, $c = 54.1$
Beamline	BL41XU			BL38B1
Resolution (Å)[a]	40–2.00 (2.11–2.00)			40–1.45 (1.50–1.45)
Wavelength (Å)	0.9792	0.9794	0.9000	0.9000
R_{sym} (%)[a,b]	6.0 (10.6)	6.2 (11.3)	5.8 (10.2)	5.2 (36.0)
Completeness (%)[a]	98.6 (99.0)	98.6 (99.0)	98.9 (99.3)	99.8 (99.7)
Observed reflections	68275	68624	69009	109978
Unique reflections	6157	6166	6154	15562
$I/\sigma(I)$	7.7	7.3	8.4	9.3
Multiplicity[a]	11.1 (11.3)	11.1 (11.3)	11.2 (11.3)	7.1 (7.2)
Refinement and model quality				
Resolution range (Å)			10–2.0	10–1.45
No. of reflections			6114	13822
Twinning fraction			0.16	–
Twinning operator			$(h\ -h\ -k\ -l)$	–
R factor[c]			0.237	0.162
R_{free} factor[d]			0.289	0.194
Total protein atoms			873	873
Total ligand atoms			0	1 (Cu^{2+})
Total water atoms			36	70
Average B factor (Å^2)			23.66	10.70
Rms deviation from ideality				
Bond lengths (Å)			0.013	0.014
Bond angles (°)			1.90	1.48
Ramachandran plot				
Residues in most favored regions (%)			89.4	94.7
Residues in additional allowed regions (%)			9.6	5.3
Residues in generously allowed regions (%)			1.1	0.0

[a]The values in parentheses refer to data in the highest-resolution shell.
[b]$R_{sym} = \Sigma_h \Sigma_i |I_{h,i} - \langle I_h \rangle| / \Sigma_h \Sigma_i |I_{h,i}|$, where $\langle I_h \rangle$ is the mean intensity of a set of equivalent reflections.
[c]R factor $= \Sigma |F_{obs} - F_{calc}| / \Sigma F_{obs}$, where F_{obs} and F_{calc} are observed and calculated structure factor amplitudes.
[d]R_{free} factor was calculated for R factor, with a random 10% subset from all reflections.

the results of gel filtration experiments (see Section 2). The surface charge of the *Pho*CutA trimer calculated using the program GRASP showed that the one site of the protein surface was relatively neutral, while its back side was negatively charged (Fig. 2B).

3.2. Crystal structure of CutA–copper complex

To elucidate the manner of interactions between protein and copper, we also determined the structure of *Pho*CutA in the presence of copper at 1.45 Å resolution. The overall structure of the *Pho*CutA–copper complex can be very well superimposed on that of unliganded *Pho*CutA with low root mean square (rms) deviation, except for narrow regions around the copper-binding site (Fig. 3A).

High-resolution structure analysis revealed that the copper ion is located at the trimer–trimer interface, at a position exactly on the crystallographic two-fold axis of symmetry (Fig. 3B). This means that one copper ion mediates the association of two *Pho*CutA trimers into a complex having two-fold symmetry. Because one trimer possesses three equivalent copper recognition sites (one site for each monomer), each trimer interacts with three neighboring trimers through the mediation of copper (Fig. 3C). Our current structure shows that copper ions are present only at intertrimer interfaces. It should be noticed that copper ion binds to the relatively neutral surface on the protein (Fig. 2A).

The copper ion is coordinated by four oxygen atoms: two crystallographically equivalent Oδ1 atoms of Asp[48] derived from each trimer and two water molecules (Fig. 3D). The distances between copper and Asp[48] Oδ1 are 1.82 Å, and between copper and the water oxygens are 1.94 Å. These four oxygen atoms and the copper are nearly coplanar. Additionally, the main chain carbonyl group of Lys[49] is located 2.74 Å from copper, roughly perpendicular to the plane of the oxygens. Thus, the copper seems to be octahedrally coordinated with six oxygen atoms. Interestingly and to the best of our knowledge, copper coordinated via only oxygen atoms has never before been observed in any solved structures of protein–copper complexes.

3.3. The mobility of PhoCutA without metal in SDS–PAGE

The mobility of *Pho*CutA without metal in SDS–PAGE is significantly lower than that of the monomer, analyzed as a trimer (Fig. 4). This suggests that the trimeric structure of hyperthermophile *Pho*CutA is very insensitive to SDS and to the near-boiling conditions we used during preparation of our samples for PAGE.

3.4. Effect of divalent metal ions on the structure of PhoCutA

To investigate the affinity of the protein for binding copper ions, various concentrations of copper ions were added to the purified *Pho*CutA. Surprisingly, the protein precipitated at 40 excess molar of metal to protein, although no aggregation was observed below the concentration (Fig. 5A). Recently, Arnesano et al. also reported a similar phenomenon for CutA from rat [36]. In addition, the precipitates were completely resolu-

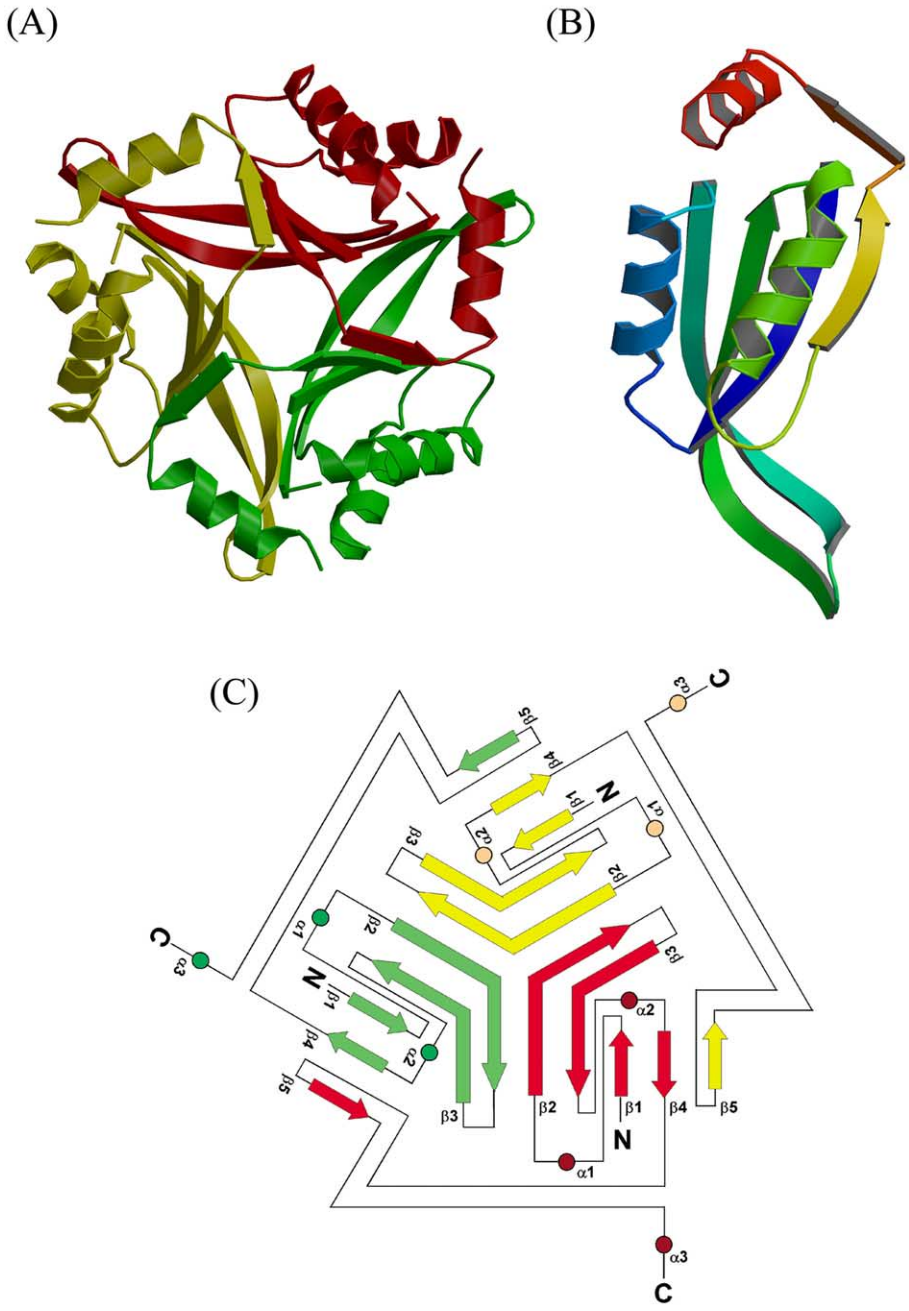

Fig. 1. Structural features of *Pho*CutA. A: Trimeric structure of *Pho*CutA. Each monomer is crystallographically related. B: Ribbon diagram of a *Pho*CutA monomer, which consists of five β-strands and three α-helices. The ribbon model is colored according to the sequence by a rainbow color ramp from blue at the N-terminus to red at the C-terminus. C: Topological diagram of trimeric structure. Arrows and circles indicate β-strands and α-helices, respectively. Intertrimer β-sheets, consisting of β1, 2, 3, and 4 in one chain, β2 and 3 in another chain, and β5 in the third chain, stabilize the trimeric structure of *Pho*CutA.

bilized by removing the metal ion by addition of ethylenediamine tetraacetic acid (EDTA) or dialysis against a solution without heavy metals (Fig. 5B). The results suggest cooperative precipitation of the protein with the metal ions.

To investigate the ability of the protein to bind other divalent cations, 20 excess molar of Mn, Ni, Co, and Zn (2 mM) were added separately to the purified CutA via dialysis. Surprisingly, the protein precipitated under these conditions (Fig. 6A). In addition, these precipitates could be rapidly resolubilized by addition of 2 mM EDTA to the solution or dialysis against a solution without heavy metals (Fig. 6B). It could be concluded, therefore, that *Pho*CutA is reversibly precipitated by divalent cations non-specifically.

Structural analyses indicated that Asp^{48} from two *Pho*CutA trimers binds the heavy metals (Fig. 3D). To address the contribution of this residue to metal ion binding, a mutant in which Asp^{48} was replaced by Ala (D48A) was constructed, and heavy metals were added to the D48A protein under the same experimental conditions as described above (Fig. 7). A decrease in the relative amount of aggregates in the presence of metal ions (except for Co) was observed, indicating the significant contribution of Asp^{48} to metal binding and

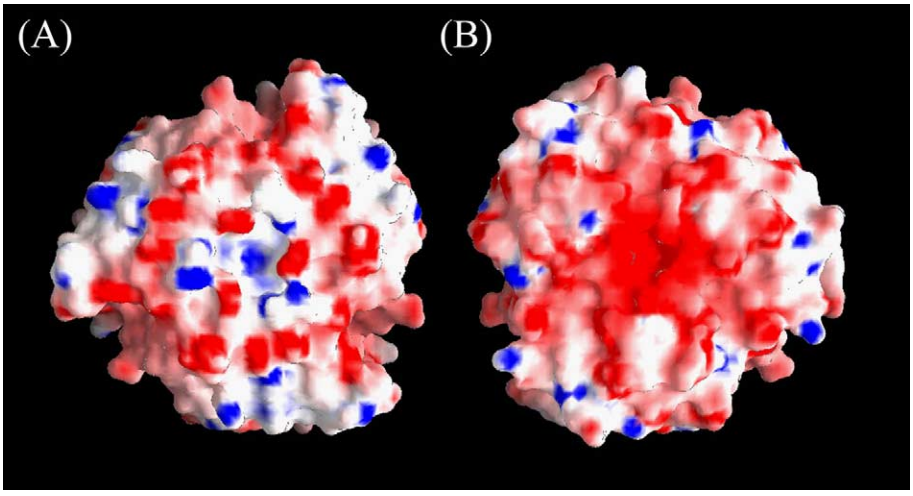

Fig. 2. Electrostatic surface representation of the two sides of the *Pho*CutA trimer. A: The view from one side of the three-fold axis of symmetry vertical to paper. Red represents negative charge, and blue positive. B: The view turned 180° around the three-fold axis from the orientation shown in A. Calculated with the program GRASP [27].

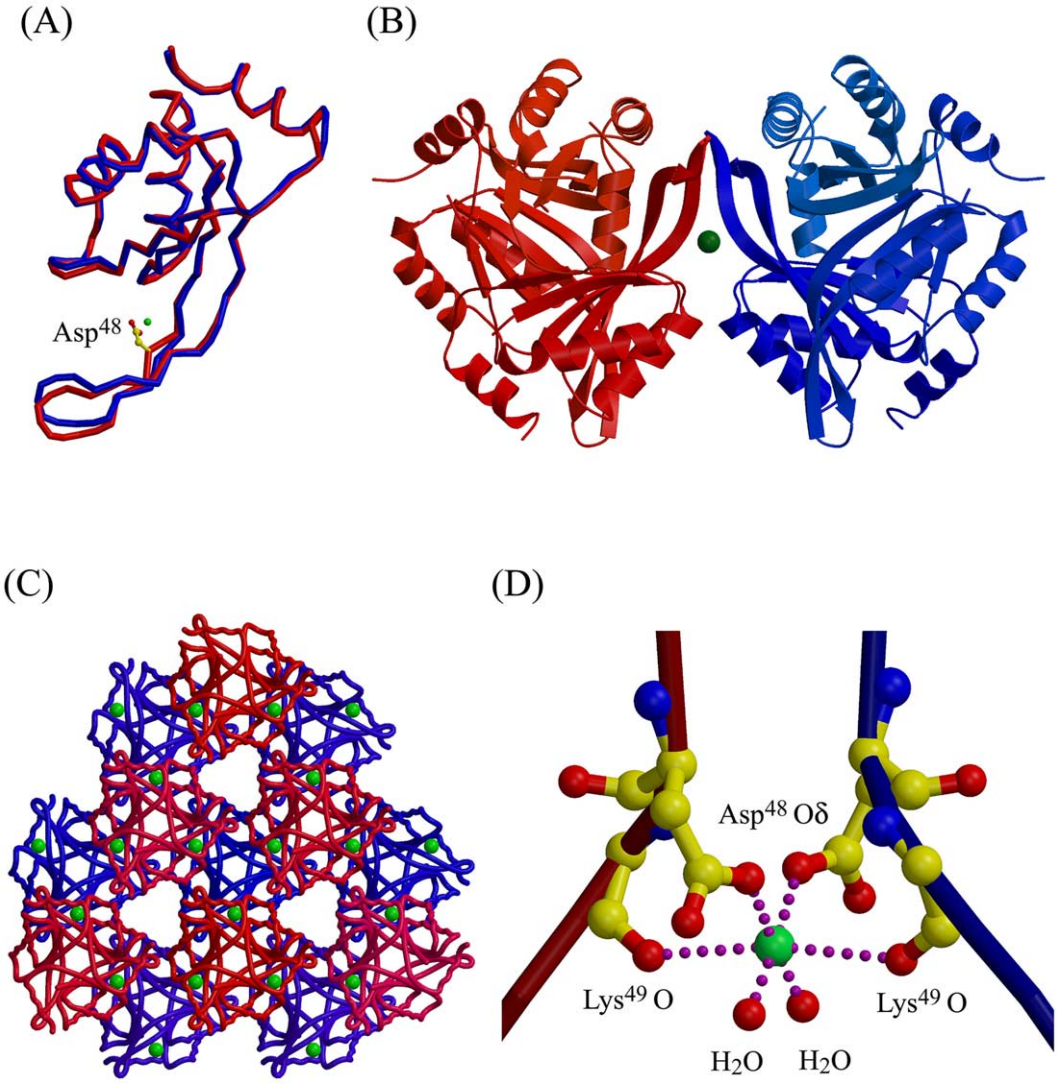

Fig. 3. Structure of *Pho*CutA complexed with copper. A: Superposition of the Cα trace of *Pho*CutA without Cu^{2+} (blue) and complexed with Cu^{2+} (red). Cu^{2+} (green ball) and Asp^{48} (ball-and-stick) are also shown. B: Ribbon diagram of dimer of trimeric structures. Copper ion (Cu^{2+}) is shown as a green ball in the trimer–trimer interface. C: Deduced structure of multimer induced by Cu^{2+} binding. Cu^{2+} is green, proteins in the first layer are blue, and proteins in the second layer are red. D: Cu^{2+}-binding site of *Pho*CutA. Each trimer is colored blue or red. Cu^{2+}-binding residues (ball-and-stick representations) and water molecules (red balls) are shown.

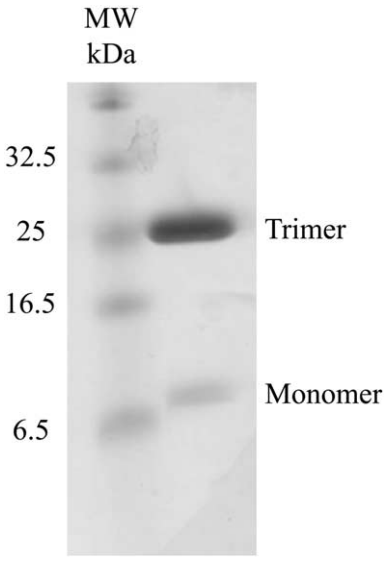

Fig. 4. SDS–PAGE of *Pho*CutA untreated by metals.

also to aggregate formation due to addition of heavy metals. With Co, however, the coordination structure of the bound metal and/or the identity of the metal-binding sites might be distinct from those with the other heavy metals, resulting in higher affinity for Co.

As described above, the mobility of *Pho*CutA without metal in SDS–PAGE is significantly lower than that of the monomer, analyzed as a trimer (Fig. 4). On the other hand, *Pho*CutA with a slight excess of certain metals ran as the monomer (Figs. 5A and 6A). In addition, removal of the divalent metal ions from the heavy metal-bound *Pho*CutA resulted in the same mobility as *Pho*CutA without metal ions, i.e. recovery of the trimeric structure (Figs. 5B and 6B). These results strongly suggest that local conformational changes in β-sheets which include Asp^{48} in response to the binding of metal ions to *Pho*CutA affect the trimeric association of the polypeptide and thus weaken to the extent as dissociate to monomer in SDS–PAGE. The conformational changes seem to be reversible, which is supported by far-ultraviolet (UV) circular dichroism spectrophotometry (data not shown). It should be noticed that the mobility of D48A mutated *Pho*CutA in SDS–PAGE is analyzed as a trimer (Fig. 7), with and without metal ions.

3.5. *Implications of metal-binding properties of* Pho*CutA*

To summarize so far, structural analysis of *Pho*CutA complexed with Cu^{2+} revealed that the metal-binding site of *Pho*CutA is Asp^{48} in the trimer–trimer interface (Fig. 3A) and that one metal ion binds to two protein molecules (Fig. 3B and C). Addition of a molar excess of Cu^{2+} to *Pho*CutA leads to aggregation of the protein, and the aggregates can be completely resolubilized by removing the metals from the solution by addition of EDTA or dialysis against a solution without heavy metal. Taken together, these results indicate that bind-

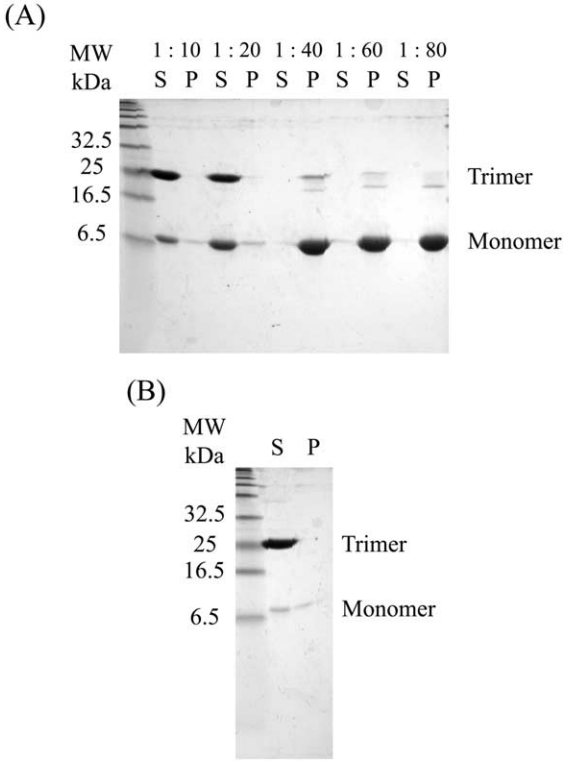

Fig. 5. Copper-induced reversible multimerization of *Pho*CutA. A: SDS–PAGE of *Pho*CutA solution (100 μM) containing several concentrations of Cu^{2+}. The molar ratio of Cu^{2+} for *Pho*CutA was described at upside of the figure. Lanes S, soluble fraction; lanes P, precipitate. B: SDS–PAGE of *Pho*CutA that had been precipitated by metal binding and was then dialyzed to remove heavy metal ions. Lanes S, soluble fraction; lanes P, precipitate.

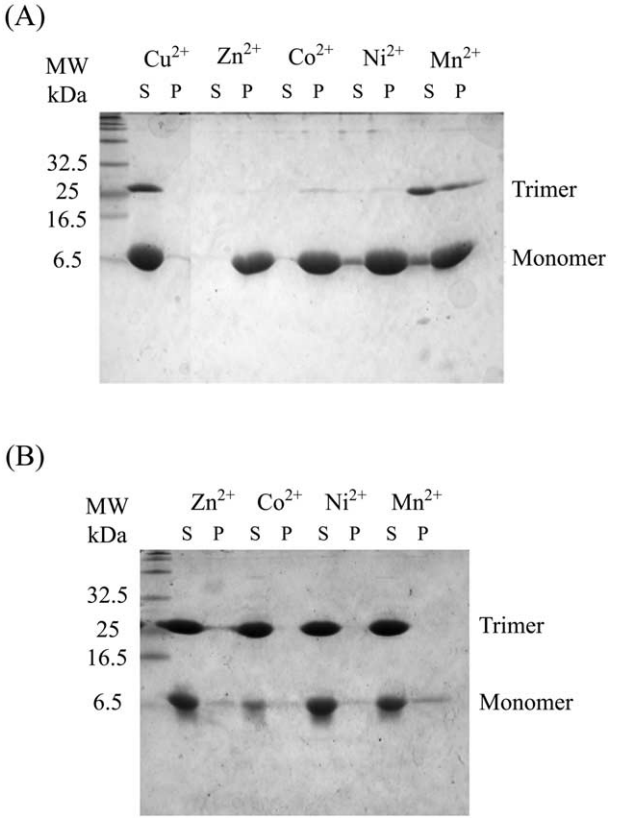

Fig. 6. Heavy metal-induced reversible multimerization of *Pho*CutA. A: SDS–PAGE of 100 μM *Pho*CutA solution containing 2 mM of the indicated heavy metal ion. Lanes S, soluble fraction; lanes P, precipitate. B: SDS–PAGE of *Pho*CutA that had been precipitated by metal binding and was then dialyzed to remove heavy metals.

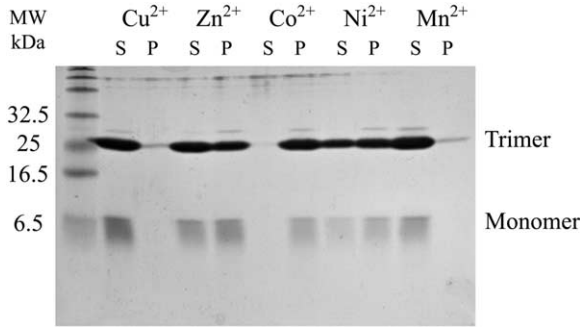

Fig. 7. SDS–PAGE of *Pho*CutA D48A mutant incubated with 2 mM of the indicated heavy metal. Lanes S, soluble fraction; lanes P, precipitate.

ing of copper ions to *Pho*CutA results in multimerization. It should be noticed that this Asp residue, of which substitution with Ala leads to a decrease in the relative amount of aggregates, is relatively conserved (Fig. 8), and that CutA from rat, which has Asp residue at the corresponding site, shows the same aggregation property [36].

Additional experiments revealed that certain other metal ions also lead to multimerization and precipitation of *Pho*CutA and that the multimers are dissociated via removal of the metal ions; i.e. multimerization is relatively non-specific and reversible. We should note that the critical metal ion concentration for causing aggregation of the protein depends on the metal (Figs. 5A and 6A), which may correlate with the affinity of metals for the protein. We should also note that *Pho*CutA has a stable trimeric structure even under conditions of 0.1% SDS and/or boiling for more than 1 h (data not shown).

Two types of proteins are known to have the same function as *Pho*CutA: one is metallothionein [28], the other are three low molecular weight proteins in *Pseudomonas putida* [29]. These proteins are Cys-rich; and the binding sites for heavy metals, especially copper, in proteins are usually constructed of Cys and/or His residues [30–33]. Recently, crystal structures of CutA from *E. coli* and rat have been reported [36]. In *E. coli* CutA, it has been suggested that Cys^{16}, His^{83} and His^{84} formed metal-binding sites from EXAFS and crystallographic analyses [36]. Corresponding residues in *Pho*CutA are Thr^{6}, Leu^{72}, and His^{73} (Fig. 8), suggesting that the metal-binding properties of *Pho*CutA are distinct from that of *E. coli*. *Pho*CutA has only one Cys and two His, which was not seen in the copper-binding site of *Pho*CutA in the crystallographic structure. The one Cys residue in *Pho*CutA is located at site 29, and the two histidine residues are located at sites 35 and 73. Cys^{29} and His^{73} are highly conserved in CutA from various sources (Fig. 8), and therefore we substituted these residues with Ala; however, the metal-induced multimerization of the protein has not been changed (data not shown), suggesting that Cys and His residues are not critical for binding to the metal or for multimerization of the protein in the case of *Pho*CutA.

In vitro multimerization of *Pho*CutA induced by heavy metal ions might be correlated with the cellular mechanism for metal resistance; i.e. *Pho*CutA may play a role in intracellular metal sequestration by capturing and precipitating intracellular heavy metals via a novel binding mechanism. This intracellular metal sequestration would prevent exposure of essential cellular components to heavy metals. To date, only one example of implementing metal resistance by precipitation of intracellular heavy metals has been found in *Mycobacterium scrofulaceum*, where CuS is accumulated as a precipitate [34]. In mammalian cells, on the other hand, a CutA-

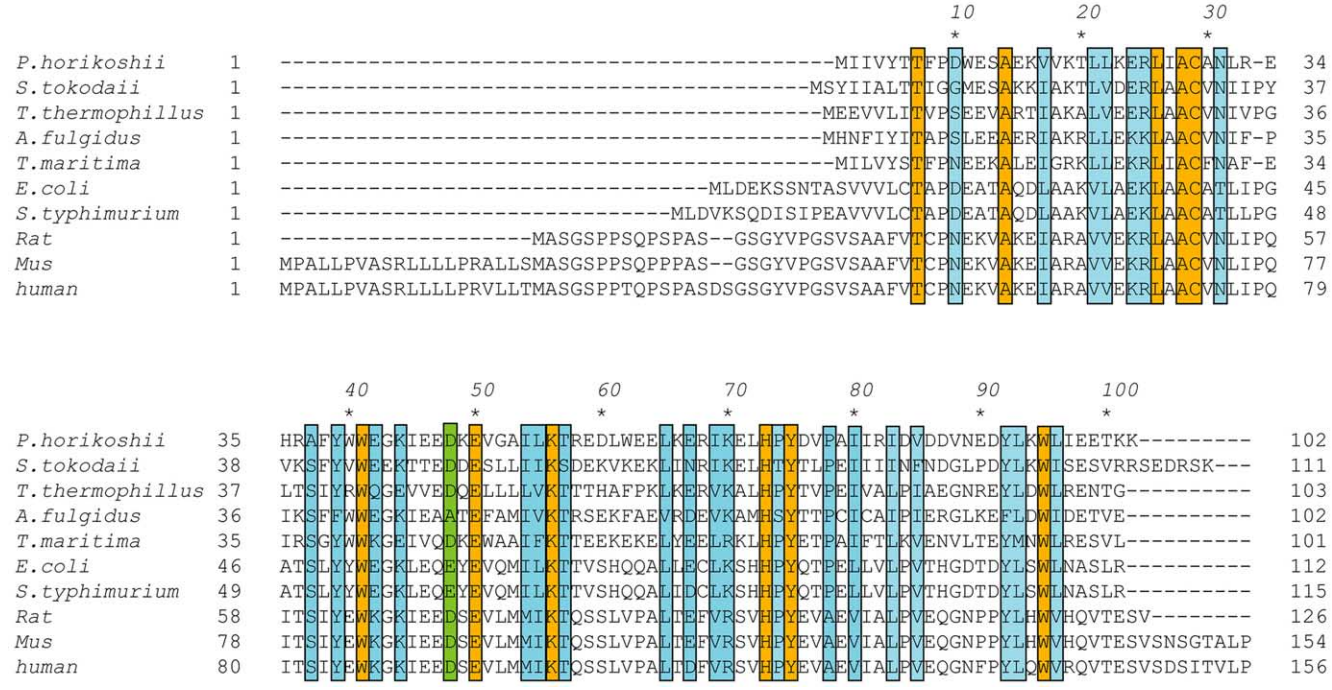

Fig. 8. Sequence alignment of CutA. The numbering for residues refers to *Pho*CutA. Completely conserved residues are highlighted in orange, and conservatively mutated sites are in light blue. Asp^{48} in *Pho*CutA and corresponding residues in other CutA molecules are boxed in green. *S. tokodaii*, *Sulfolobus tokodaii*; *T. thermophilus*, *Thermus thermophilus*; *A. fulgidus*, *Archaeoglobus fulgidus*; *T. maritima*, *Thermotoga maritima*; *S. typhimurium*, *Salmonella typhimurium*; *Rat*, *Rattus norvegicus*; *Mus*, *Mus musculus*; *human*, *Homo sapiens*.

like protein, acetylcholine esterase related protein, has been proposed to have some role in the transport of ligands to membranes [35]. Further investigation of the protein from proteomics viewpoints should give critical insights into the function of *Pho*CutA. Finally, we want to emphasize that, to the best of our knowledge, this is the first report which provides the structural evidence for heavy metal-induced multimerization of a protein perhaps due to location of metal ions on the protein surface. Therefore, the proposed structure reported here may constitute a new structural model for metal-responsive assembly of proteins lacking Cys and His residues.

Acknowledgements: This work was supported in part by the National Project on Protein Structural and Functional Analyses from the Ministry of Education, Culture, Sports, Science and Technology of Japan. It was also partially supported by the Ministry of Education, Culture, Sports, Science and Technology by a Grant-in-Aid for the COE project, Giant Molecules and Complex Systems, 2002. We thank M. Kawamoto, Dr. H. Sakai, and Dr. K. Miura of the Japan Synchrotron Radiation Research Institute (JASRI) for their help with the X-ray diffraction experiments at SPring-8.

References

[1] Harris, E.D. (1992) J. Nutr. 122, 636–640.
[2] Ochiai, T., Hoshina, S. and Usuki, I. (1993) Biochim. Biophys. Acta 1203, 310–314.
[3] Ji, G. and Silver, S. (1995) J. Ind. Microbiol. 14, 61–75.
[4] Nies, D.H. (1999) Appl. Microbiol. Biotechnol. 51, 730–750.
[5] Bruins, M.R., Kapil, S. and Oehme, F.W. (2000) Ecotoxicol. Environ. Saf. 45, 198–207.
[6] Silver, S. and Phung, L.T. (1996) Annu. Rev. Microbiol. 50, 753–789.
[7] Odermatt, A., Suter, H., Krapf, R. and Solioz, M. (1993) J. Biol. Chem. 268, 12775–12779.
[8] Odermatt, A. and Solioz, M. (1995) J. Biol. Chem. 270, 4349–4354.
[9] Brown, N.L., Lee, B.T.O. and Silver, S. (1994) in: Metal Ions in Biological Systems (Sigel, H. and Sigel, A., Eds.), Vol. 30, pp. 405–434, Marcel Dekker, New York.
[10] Rogers, S.D., Bhave, M.R., Mercer, J.F., Camakaris, J. and Lee, B.T.O. (1991) J. Bacteriol. 173, 6742–6748.
[11] Gupta, S.D., Gan, K., Schmid, M.B. and Wu, H.C. (1993) J. Biol. Chem. 268, 16551–16556.
[12] Gupta, S.D., Lee, B.T.O., Camakaris, J. and Wu, H.C. (1995) J. Bacteriol. 177, 4207–4215.
[13] Snyder, W.B., Davis, L.J., Danese, P.N., Cosma, C.L. and Silhavy, T.J. (1995) J. Bacteriol. 177, 4216–4223.
[14] Fong, S.T., Camakaris, J. and Lee, B.T.O. (1995) Mol. Microbiol. 15, 1127–1137.
[15] Leslie, A.G.W. (1992) in: Joint CCP4 and ESF_EAMBC Newsletter on Protein Crystallography, p. 26, SERC Daresbury Laboratory, Warrington.
[16] Collaborative Computational Project, Number 4 (1994) Acta Crystallogr. Sect. D Biol. Crystallogr. 50, 760–763.
[17] Chandra, N., Acharya, K.R. and Moody, P.C.E. (1999) Acta Crystallogr. Sect. D Biol. Crystallogr. 55, 1750–1758.
[18] Brunger, A.T., Adams, P.D., Clore, G.M., DeLano, W.L., Gros, P., Grosse-Kunstleve, R.W., Jiang, J.-S., Kuszewski, J., Nilges, M., Pannu, N.S., Read, R.J., Rice, L.M., Simonson, T. and Warren, G.L. (1998) Acta Crystallogr. Sect. D Biol. Crystallogr. 54, 905–921.
[19] Murshudov, G.N., Vagin, A.A. and Dodson, E.J. (1997) Acta Crystallogr. Sect. D Biol. Crystallogr. 53, 240–255.
[20] Otwinowski, Z. and Barendzen, J. (1997) Methods Enzymol. 276, 307–326.
[21] Terwilliger, T.C. and Barendzen, J. (1999) Acta Crystallogr. Sect. D Biol. Crystallogr. 55, 849–861.
[22] Terwilliger, T.C. and Barendzen, J. (1999) Acta Crystallogr. Sect. D Biol. Crystallogr. 55, 1872–1877.
[23] Terwilliger, T.C. (2000) Acta Crystallogr. Sect. D Biol. Crystallogr. 56, 965–972.
[24] Jones, T.A., Zou, J.Y., Cowan, S.W. and Kjeldgaard, M. (1991) Acta Crystallogr. Sect. A 47, 110–119.
[25] Navaza, J. (1994) Acta Crystallogr. Sect. A 50, 157–163.
[26] Laskowski, R.A., MacArthur, M.W., Moss, D.S. and Thornton, J.M. (1993) J. Appl. Crystallogr. 26, 283–291.
[27] Nicholls, A., Sharp, K. and Honig, B. (1991) Proteins Struct. Funct. Genet. 11, 281–296.
[28] Turner, J.S. and Robinson, N.J. (1995) J. Ind. Microbiol. 14, 119–125.
[29] Higham, D.P., Sadler, P.J. and Scawen, M.D. (1986) Environ. Health Perspect. 65, 5–11.
[30] Harding, M.M. (2001) Acta Crystallogr. Sect. D Biol. Crystallogr. 57, 401–411.
[31] Fusetti, F., Schroter, K.H., Steiner, R.A., Noort, P.I.V., Pijning, T., Rozeboom, H.J., Kalk, K.H., Egmond, M.R. and Dijkstra, B.W. (2002) Structure 10, 259–268.
[32] Harata, K., Schubert, W.D. and Muraki, M. (2001) Acta Crystallogr. Sect. D Biol. Crystallogr. 57, 1513–1517.
[33] Opella, S.J., DeSilva, T.M. and Veglia, G. (2002) Curr. Opin. Chem. Biol. 6, 217–223.
[34] Mergeay, M. (1991) Trends Biotechnol. 9, 17–24.
[35] Perrier, A.L., Cousin, X., Boschetti, N., Haas, R., Chatel, J.M., Bon, S., Roberts, W.L., Pickett, S.R., Massoulie, J., Rosenberry, T.L. and Krejci, E. (2000) J. Biol. Chem. 275, 34260–34265.
[36] Arnesano, F., Banci, L., Benvenuti, M., Bertini, I., Calderone, V., Mangani, S. and Viezzoli, M.S. (2003) J. Biol. Chem. 278, 45999–46006.